

Aerosol oxalate and its implication to haze pollution in Shanghai, China

Yilun Jiang · Guoshun Zhuang · Qiongzen Wang · Tingna Liu · Kan Huang · Joshua S. Fu · Juan Li · Yanfen Lin · Rong Zhang · Congrui Deng

Received: 17 March 2013 / Accepted: 29 August 2013 / Published online: 31 December 2013
© Science China Press and Springer-Verlag Berlin Heidelberg 2013

Abstract A total of 238 samples of PM_{2.5} and TSP were analyzed to study the characteristics, sources, and formation pathways of aerosol oxalate in Shanghai in four seasons of 2007. The concentrations of oxalate were 0.07–0.41 μg/m³ in PM_{2.5} and 0.10–0.48 μg/m³ in TSP, respectively. Oxalate displayed a seasonal variation of autumn > summer > winter > spring in both PM_{2.5} and TSP and was dominantly present in PM_{2.5} in all samples. Correlation between oxalate and K⁺ and high ratio of oxalate/K⁺ suggested that biomass burning was a secondary source of aerosol oxalate in Shanghai, in addition to urban VOCs sources (vehicular and industrial emissions), especially in autumn. Secondary formation accounted for the majority of aerosol oxalate in Shanghai, which was supported by the high correlation of oxalate with nss-SO₄²⁻, K⁺ and NO₃⁻, proceeding from different mechanisms. Relatively high ambient RH together with high cloud cover was found benefiting the secondary formation of aerosol oxalate. The in-cloud process (aqueous-phase oxidation) was proposed to be likely the major formation pathway of aerosol oxalate in Shanghai, which was supported by the high correlation of oxalate with nss-SO₄²⁻ and K⁺, dominant residence of oxalate in droplet mode and result of favorable meteorological condition analysis. High correlation of oxalate and NO₃⁻ reflected the OH radical

involved oxidation chemistry of the two species in the atmosphere and also suggested that gas-particle surface reactions and the evaporation–condensation process were both possible secondary formation pathways of aerosol oxalate in coarser particle mode (>1.0 μm). As a major water-soluble organic compound in aerosols, concentration of oxalate showed a distinct negative correlation to the atmospheric visibility, which implied that aerosol organic compounds could play an important role in haze pollution as well as in air quality in Shanghai.

Keywords Aerosol oxalate · Source apportionment · Formation pathway · Haze pollution · Visibility · Organic aerosol

1 Introduction

Oxalic acid, with oxalate, has attracted a great deal of attention as the most abundant dicarboxylic acid in the tropospheric aerosols [1–3]. As a major identified water-soluble organic compound in aerosol, oxalate could affect hygroscopic properties of aerosol particles [4, 5]. It can act as cloud condensation nuclei (CCN) or reduce the surface tension of particles to form CCN [6–8]; the refractive index of aerosol particles can be influenced by the presence of oxalate and further their radiative-forcing estimates. Oxalate may also play a role in solubility, photochemistry, and bioavailability of transition metals in aerosols [9].

The sources and formation pathways of aerosol oxalate are still under investigation. Oxalate can be emitted directly from fossil fuel combustion, biomass burning, and biogenic activity. However, many studies suggested the existence of a global secondary source in addition to the primary sources of the compound [10, 11]. A large fraction

Y. Jiang · G. Zhuang (✉) · Q. Wang · T. Liu · K. Huang · J. Li · Y. Lin · R. Zhang · C. Deng
Center for Atmospheric Chemistry Study, Department of Environmental Science and Engineering, Fudan University, Shanghai 200433, China
e-mail: gzhuang@fudan.edu.cn

K. Huang · J. S. Fu
Department of Civil and Environmental Engineering,
The University of Tennessee, Knoxville, TN 37996, USA

of aerosol oxalate is considered to be produced from radical involved chemical/photochemical oxidation of volatile organic compounds (VOCs) like ethene, toluene, isoprene, etc. [12, 13]. Based on some observations, the maximum oxalate concentrations appeared in the droplet mode at 0.54–1.0 μm with MMAD (mass median aerodynamic diameters) at 1.0 μm [14]. In-cloud process and oxidation of gaseous precursors followed by condensation are the two major suggested secondary formation pathways of aerosol oxalate in the fine particle mode [15–18]. A close tracking of oxalate and sulfate in the atmosphere has been observed in some studies, which suggested a similar dominant formation pathway of the two chemically distinct species [19, 20]. Martinelango et al. [21] discovered parallel formation pathways of oxalate and nitrate in a coastal atmosphere.

Shanghai (31°13'N, 121°28'E) is located in the western coast of the North Pacific Ocean, east front of the Yangtze River Delta, China. It is one of the largest, urbanized and motorized cities in China with a population of $\sim 19,000,000$. Shanghai has the marine monsoon subtropical climate with an annual average precipitation of $\sim 1,100$ mm (<http://cdc.cma.gov.cn>). Under the influence of the monsoon system, 1 year in Shanghai is usually divided into the hiemal half-year from November to April with prevailing northwesterly continental wind and the estival half-year from May to October with prevailing southeasterly wind from the North Pacific Ocean [22]. For the past decade the air quality has been terribly degraded due to the rapid motorization, and the heavy haze has been the frequent weather pattern in Shanghai. Organic acids, including oxalic acid, with the organic aerosol have been considered as one of major components of haze. In this paper we report the concentration levels, seasonal variation and relative distribution of aerosol oxalate in $\text{PM}_{2.5}$ and TSP, as well as the possible sources and formation pathways of aerosol oxalate. The relationships between oxalate, meteorological factors, and the regional haze pollution are also discussed. This is the first time the sources and the formation pathway of aerosol oxalate in Shanghai, the eastern Asian megacity, were systematically investigated. The role of organic aerosol in urban atmospheric haze pollution was explored through this water-soluble organic acid in aerosols.

2 Experimental

2.1 Sampling

Aerosol samples of $\text{PM}_{2.5}$ and TSP were collected in four seasons in 2007 in Shanghai. The sampling site was on the roof (~ 15 m) of a building at Fudan University, located in the urban area of Shanghai. Samples were collected on

Whatman® 41 polycarbonate filters (Whatman Inc., Maidstone, UK, diameter: 90 mm) by a medium-volume sampler (Model: (TSP/ PM_{10} / $\text{PM}_{2.5}$)-2, flow rate: 76.67 L min^{-1}). Sampling was carried out approximately in 24-h intervals. The sampling periods were chosen to represent different seasons: (1) March 20–April 20, 2007: spring; (2) July 23–August 19, 2007: summer; (3) November 1–November 29, 2007: autumn; and (4) December 24, 2007–January 26, 2008: winter. Polycarbonate filters were put in the sampler at the sampling site for 24 h (without pumping) and used as the blanks. Four blanks were collected in every season. Samples were placed in polyethylene plastic bags with artificial parchment lining bags right after sampling and reserved in a refrigerator (-18 °C). All of those filters were weighed before and after sampling with an analytical balance (Sartorius 2004 MP, reading precision 10 μg) after stabilizing under constant temperature (20 ± 1 °C) and humidity ($40 \% \pm 2 \%$). A total of 238 aerosol samples were collected and used in this study. All the procedures were strictly quality-controlled to avoid any possible contamination of the samples.

Black carbon (BC) measurement was conducted before a series of chemical analysis. The concentration of BC in the aerosol samples was measured by a smoke stain reflectometer (model 43D, Diffusion Systems Ltd., London, UK). Five spots on each complete sample filter were selected randomly and evenly as possible for the measurement of BC contents which were calculated from comparing the reflectance of the sample filter with that of a clean filter [23].

2.2 Ion analysis and pH measurement

One-fourth of each aerosol sample filter and blank filter was extracted ultrasonically by 10 mL water, which was deionized to the resistivity of 18 $\text{M}\Omega \text{cm}^{-1}$. After passing through the microporous membranes (mixed cellulose, pore size, 0.45 μm ; diameter, 25 mm), each filtrate was stored at 4 °C in a clean tube for analysis. The concentrations of ten anions (F^- , CH_3COO^- , HCOO^- , MSA, Cl^- , NO_2^- , NO_3^- , SO_4^{2-} , $\text{C}_2\text{O}_4^{2-}$, PO_4^{3-}) and five cations (Na^+ , NH_4^+ , K^+ , Mg^{2+} , Ca^{2+}) in the aqueous extracts were determined by ion chromatography (IC, Dionex 3000, USA). The gradient base eluent (76.2 mmol/L NaOH + H_2O) was used for anion detection, while the weak acid eluent (20 mmol/L MSA) for cation detection. The oxalate concentrations of the blanks were below detection limit or under 0.02 $\mu\text{g}/\text{m}^3$ and had been deducted from the observation values. The recovery of ions was in the range of 80 %–120 % by adding standard reference material of each ion component to the filtrates for ion chromatography analysis. Reproducibility test showed that relative standard

deviation was less than 5 % by calculating from the results of ion chromatography detections of one sample at different times (under same analytical condition). The quality assurance was routinely carried out by using Standard Reference Materials produced by National Research Center for Certified Reference Materials, China. A pH meter (model: LIDA PHS-2C) combined with a glass electrode was used for pH measurement of the filtrates for ion chromatography analysis. The pH meter was calibrated before measurement using standard buffer solutions with pH values of 4.00 and 6.86. Detailed procedures were given elsewhere [24].

2.3 Element analysis

Half of the sample and blank filter was digested at 170 °C for 4 h in high-pressure Teflon digestion vessel with 3 mL concentrated HNO₃, 1 mL concentrated HCl, and 1 mL concentrated HF. After cooling, the solutions were dried, then by adding 0.1 mL concentrated HNO₃ to them, they were diluted to 10 mL with MilliQ water (resistivity of 18 MΩ cm⁻¹). A total of 19 elements (Al, Fe, Mn, Mg, Ti, Sc, Na, Sr, Ca, Co, Cr, Ni, Cu, Pb, Zn, Cd, V, S, and As) were determined by inductively coupled plasma atomic emission spectroscopy (ICP-AES, Model: ULTIMA, JOBIN–YVON Company, France). The detailed analytical procedures were given elsewhere [25, 26]. Al was used as the reference element of crustal source in this study.

2.4 Meteorological Conditions and Sampling Artifact

Meteorological data, including temperature, relative humidity (RH), cloud cover, wind speed, visibility, and atmospheric pressure were downloaded from <http://www.arl.noaa.gov> and <http://www.wunderground.com>. The daily average concentrations of ambient gaseous SO₂ and NO₂ in Shanghai were obtained from <http://www.semc.gov.cn>.

The extent of the sampling artifact strongly depended on the volatility of the compounds, the aerosol acidity, the ambient temperature, and relative humidity [27, 28]. The vapor pressure of oxalate is <20 mmHg at 20 °C which

reflects a low volatility of this compound. Low ambient temperature, low aerosol acidity and high relative humidity would make oxalate in the atmosphere more associated with particles. The aerosols in Shanghai are known to be acidic due to the high concentration of SO₂ and NO_x [29]. Results of our measurement also showed that the pH of aerosol filtrates in Shanghai averaged at 3.96–5.41 (Table 1). However, the temperature of the ambient atmosphere in Shanghai was moderate except in summer and the average RH was above 65 % throughout the year. Consequently, the oxalate detected in the aerosol samples are expected to be able to represent the characteristics of the majority of the atmospheric oxalate and its measurement in this work is considered not affected by sorption or desorption artifacts under the local condition of Shanghai.

3 Results and discussion

3.1 Characteristics of aerosol oxalate in Shanghai

3.1.1 Concentration level, seasonal variation, and relative distribution of oxalate in PM_{2.5} and TSP

Average concentrations of oxalate in Shanghai in both PM_{2.5} and TSP are presented in Table 2. For comparison, oxalate mass concentrations of some other sites over the world are also listed in Table 2.

The oxalate concentrations in Shanghai in 2007 sampling year were 0.07–0.41 μg/m³ in PM_{2.5} and 0.10–0.48 μg/m³ in TSP, respectively. The oxalate concentrations in PM_{2.5} were a little lower than the value measured in 1999–2000 by Yao et al. [30]. Table 2 shows that the concentrations of oxalate in Shanghai were lower than those in Beijing and Hong Kong, but comparable to those in Nanjing, Tokyo, Chiba, Tampa Bay, and LA. The higher levels of oxalate in Beijing may be explained by its heavy traffic emissions and winter heating system, while the high relative humidity and thick cloud cover may be responsible for the high values in Hong Kong.

Table 1 Average aerosol pH values, ambient relative humidity, temperature, SO₂, and NO₂ concentrations in the four sampling seasons in Shanghai

	pH		Relative humidity (%)	Temperature (°C)	SO ₂ (mg/m ³)	NO ₂ (mg/m ³)
	PM _{2.5}	TSP				
Spring	3.96 (2.92–4.57)	4.35 (3.61–5.97)	66.0 (50–87)	15.5 (8–22)	0.070 (0.026–0.173)	0.060 (0.022–0.091)
Summer	5.25 (3.77–6.04)	6.22 (5.91–6.33)	71.4 (60–80)	30.8 (28–34)	0.056 (0.020–0.119)	0.042 (0.013–0.096)
Autumn	5.41 (4.00–5.99)	6.41 (6.16–6.65)	65.6 (53–83)	13.7 (8–18)	0.051 (0.022–0.096)	0.058 (0.023–0.103)
Winter	5.25 (3.81–6.06)	5.44 (4.24–6.33)	70.6 (44–90)	5.5 (0–12)	0.075 (0.011–0.203)	0.59 (0.014–0.130)

The ranges of all parameters in the brackets were based on daily average values

Table 2 Aerosol oxalate concentrations measured at different sampling sites around the world

Site	Sampling period	Size	Concentration ($\mu\text{g}/\text{m}^3$)	References
Shanghai	March 2007–January 2008	PM _{2.5}	0.07–0.41	This work
Shanghai	1999–2000	PM _{2.5}	0.50	[30]
Nanjing	2001	PM _{2.5}	0.22–0.30	[31]
Hong Kong	Winter 2000	PM _{2.5}	0.35 \pm 0.14	[32]
Tokyo	1989	PM _{2.5}	0.27 \pm 0.19	[1]
Beijing	2002–2003	PM _{2.5}	0.35 \pm 0.26	[33]
Shanghai	March 2007–January 2008	TSP	0.10–0.48	This work
Tokyo	February 1992	TSP	0.27 \pm 0.19	[34]
Chiba	April 1987–March 1993	TSP	0.38	[35]
Tampa Bay	2002	PM _{12.5}	0.29	[21]
Los Angeles	1984	TSP	0.19 \pm 0.78	[36]
Beijing	2002–2003	PM ₁₀	0.38 \pm 0.32	[33]

Table 3 Seasonal variations of the oxalate concentrations ($\mu\text{g}/\text{m}^3$) and their contributions (%) to the total mass of the aerosols

	Spring	Summer	Autumn	Winter	Dust day April 2, 2007
PM _{2.5}					
Mean	0.14	0.20	0.31	0.15	0.26
Median	0.12	0.13	0.29	0.11	
Contribution	0.59	0.80	0.77	0.13	0.21
TSP					
Mean	0.19	0.27	0.37	0.25	0.67
Median	0.12	0.25	0.36	0.15	
Contribution	0.19	0.49	0.38	0.10	0.09

Level of significance: 95 %

The seasonal variation of oxalate concentrations in PM_{2.5} and TSP samples collected in 2007 is shown in Table 3. The average concentrations of oxalate indicated a seasonal variation of autumn > summer > winter > spring in both PM_{2.5} and TSP. Their contributions to the total mass of the aerosols displayed in a slightly different order as summer > autumn > spring > winter. Since the production of aerosol oxalate in the atmosphere is generally a radical (mainly hydroxyl radical) related photo-oxidation or chemical oxidation process [20, 21], the high concentrations of oxalate in summer and autumn can be attributed to the generally high ambient temperature and more solar radiation in these two seasons.

The relative distribution of oxalate and several selected inorganic ions between PM_{2.5} and TSP in each season was analyzed. As shown in Fig. 1, oxalate was mainly present in the fine particle mode. The value of PM_{2.5}/TSP of oxalate concentration reached its peak in summer, up to 0.88. According to the data of our online PM_{2.5} and PM₁ monitoring in the same sampling site, the ratios of mass

concentration of PM₁ to that of PM_{2.5} averaged at 80 % in 2009 in Shanghai which suggested that aerosol oxalate probably dominated in finer particles (<1.0 μm). This is consistent with the results of previous studies, in which the majority of aerosol oxalate was found appeared in the accumulation mode (0.1–2.0 μm) with a MMAD around 1.0 μm , while small fraction of it distributed in the coarse mode (>2.0 μm) and Aitken mode (<0.1 μm) [14, 21].

It could also be seen clearly in Fig. 1 that nss-sulfate (non-sea salt sulfate), ammonium, and potassium reside dominantly in PM_{2.5} rather than in TSP in all four seasons, with an exception of nitrate. The ratios of PM_{2.5} to TSP of nitrate concentration were near to 0.5 which may be explained by the high volatility of nitric acid/nitrate and the coastal environment of Shanghai. Gaseous nitric acid (HNO₃) and nitrate (NO₃⁻) bound to aerosol particles coexist in the atmosphere. Nitrate in the aerosols can exist in the forms of NH₄NO₃, NaNO₃, Ca(NO₃)₂, etc., depending on the category and concentration of gaseous and aerosol species which nitric acid can obtain to combine with. In the coastal area, the abundant atmospheric sea salt aerosols can partition gas-phase nitric acid to particle- or aqueous-phase NaNO₃ [37]. Most of the newly formed NaNO₃ still reside in coarse particles of sea salt which consequently decreased the PM_{2.5}/TSP ratio of nitrate in Shanghai. Martinelango et al. [21] indicated a high ratio of PM₁₀/PM_{2.5} of nitrate in a coastal environment, while studies carried out in Hong Kong also observed a dominant coarse mode of nitrate [38]. More nitric acid would partition to gas-phase under hot and acidic ambient environment, which means more coarse mode nitrate could be produced from the gas-phase through the sea salt conversion. From our observation, the two lowest PM_{2.5}/TSP ratios of nitrate appeared in spring, the most acidic season, and in summer, the season with the highest temperature, lend more support to this viewpoint.

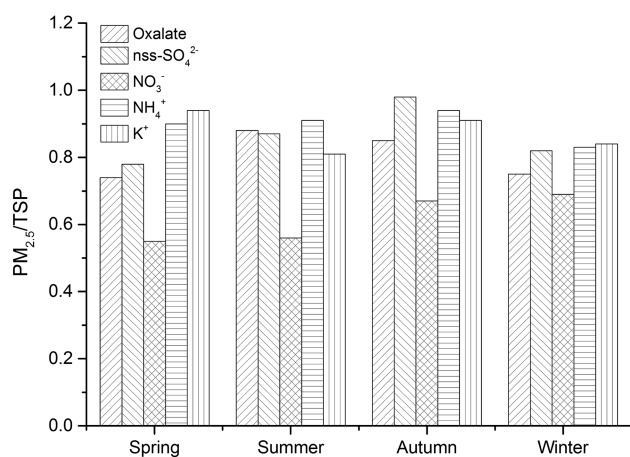


Fig. 1 Distribution of aerosol oxalate and selected inorganic ions between PM_{2.5} and TSP in four seasons of Shanghai

The probable dominant droplet mode oxalate and similarity in size distribution between oxalate and the inorganic ions also gave suggestion on the sources and formation pathways of aerosol oxalate which would be discussed further in the following sections.

3.1.2 Case study

Aerosol oxalate in a dust event. In an ever-recorded dust day on April 2, 2007, sampling was segmented to five periods (Table 4) to avoid possible overload of the filters and to gain a more lucid profile of the dust event. The most intensive input of the dust occurred in the morning time (09:29–12:10) in which the mass concentration of TSP and oxalate in TSP rushed to 1340.4 and 1.14 $\mu\text{g}/\text{m}^3$, respectively. At the same time, the PM_{2.5}/TSP ratio of mass and oxalate concentration decreased to 0.29 and 0.38, which was nearly half of the values in normal days. The three-day back trajectories exhibited the air mass movements at the beginning of the dust day (Fig. 2a). The dust air mass originated from west/northwest China, where is a major source area of Asian dust, crossed the continent to the coastal regions, over the Bohai Sea and the Yellow Sea and finally arrived at Shanghai. The transport heights of the air mass were at 2500–3500 m, which were typical of the high altitude transport weather pattern of a dust event. The aerosols arrived at Shanghai were mixed aerosols formed by interactions between the dust particles, the anthropogenic pollutants entrained along the transport pathway and at local areas, and the gaseous species and sea salts over the seas. However, dust particles still took the bulk of the total mass of the ambient aerosols on the dust day in Shanghai (Table 4).

During the transport of the dust aerosols, atmospheric oxalate and its precursors over the continent and the seas

could be entrained and reacted with the alkaline/neutral components in the dust aerosols, which led to increase in the absolute content of oxalate in the dust plume as well as redistributions of atmospheric oxalate from gaseous phase or fine particle mode to the predominant and more alkaline coarse particle mode. This could explain the distinct decrease of PM_{2.5}/TSP ratio of oxalate concentration during the dust episode compared to the value of spring average.

Intensity of the dust lessened gradually along the time which could be concluded from the aerosol mass concentrations in the five successive sampling periods. The mass concentrations of both PM_{2.5} and TSP in the fifth period (22:29 April 2–09:11 April 3) displayed an obvious decline, suggesting the ending of this dust event. Air masses observed largely came from north China instead and the transport heights were obviously lower than those at the beginning of the dust event (Fig. 2b). The cloud cover, which was believed to be influenced by the Asian brown cloud (ABC) arisen by the dust air mass to a great extent in this case, also decreased from 104 to 66.7 PCT at the ending. However, the PM_{2.5}/TSP ratio of aerosol mass and oxalate concentration changed differently to the concentrations themselves. They both reached the minimums at the third period (15:19–19:42) of the sampling, in which the ratios were 0.11 for mass concentration and 0.31 for oxalate concentration, respectively. Then in the fourth and fifth periods, the ratios kept rising back to the normal day level. This was in accordance with the fact that dust aerosol was mainly composed of coarse particles and the relative concentration of the coarse particles measured in downwind area would decrease with the weakening of the dust event. Less input of coarse mode particles meant that the aerosol oxalate from local primary/secondary sources, which was mainly resided in fine particle mode in Shanghai, began taking up the predominance.

3.2 Possible sources and formation pathways of aerosol oxalate in Shanghai

3.2.1 Source identification by correlation analysis

To explore the possible sources and formation pathways, oxalate together with some species, which could be the indicator or the tracer of the various sources, was subjected to correlation analysis. We selected Al as the indicator for the crustal source, NO₂⁻ for vehicular emission, nss-SO₄²⁻ and NO₃⁻ for secondary formation through different pathways, and K⁺ for biomass burning. The correlation coefficients between these source-indicating species and oxalate in PM_{2.5} are listed in Table 5.

Aerosol oxalate exhibited a poor correlation with aluminum with a peak value in spring ($r = 0.02\text{--}0.53$,

Table 4 Segmented aerosol and oxalate mass concentrations, $PM_{2.5}/TSP$ ratio, and the meteorological parameters on April 2, 2007

Time (UTC + 0800)	Mass concentration ($\mu\text{g}/\text{m}^3$)			Oxalate concentration ($\mu\text{g}/\text{m}^3$)			Ambient temperature ($^{\circ}\text{C}$)	Cloud cover (PCT)
	$PM_{2.5}$	TSP	$PM_{2.5}/TSP$	$PM_{2.5}$	TSP	$PM_{2.5}/TSP$		
09:29–12:10	383.3	1340.4	0.29	0.43	1.14	0.38	11.9	104
12:14–15:14	223.8	1221.0	0.18	0.32	0.99	0.32	13.1	104
15:19–19:42	101.5	913.9	0.11	0.24	0.76	0.31	11.7	104
19:46–22:21	92.0	449.4	0.20	0.19	0.35	0.55	8.6	104
22:29–09:11	35.4	106.2	0.33	0.10	0.12	0.85	6.8	66.7
Spring average ^a	47.9	95.6	0.50	0.14	0.19	0.74	15.5	47.7

^a Based on daily average values in spring sampling campaign, the dust day not included

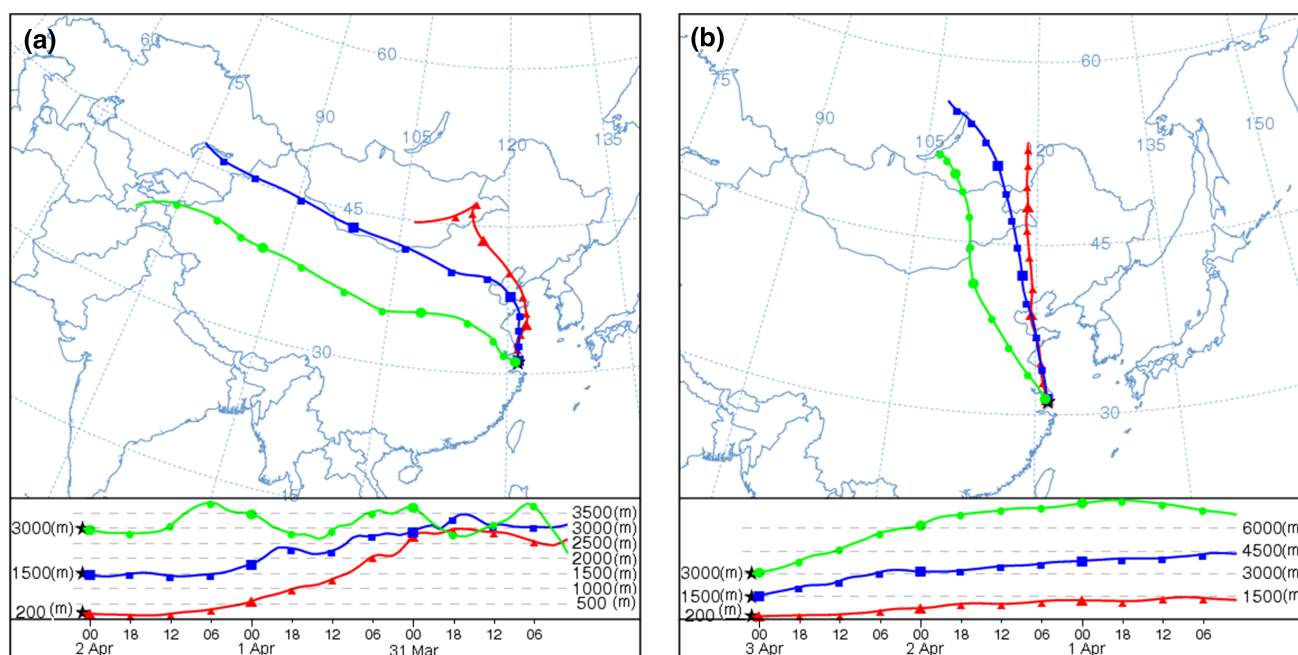
**Fig. 2** The 72-h back trajectories of air masses at the beginning (a) and the ending (b) of the dust day in Shanghai

Table 5). This suggested the contribution from crust or soil to the atmospheric oxalate mass in Shanghai was relatively small. A moderate correlation coefficient of 0.53 between oxalate and Al in spring could be brought by a larger amount of dust/soil aerosol input from north/northwest areas of China to the coastal region in this season. Emissions of oxalate or its precursors from the metabolic processes of various soil fungal species could be another explanation for such a trend of correlation coefficients between oxalate and Al along the seasons. Obviously higher values were observed in spring ($r = 0.53$) and summer ($r = 0.36$) than in autumn ($r = 0.02$) and winter ($r = 0.10$), which was the inactive period of the metabolic processes of plants (Table 5).

Previous researches suggested that combustion processes were important sources of atmospheric HNO_2 and

the most effective source of this type was the automobile engine [33, 39]. The concentrations of nitrite (NO_2^-) associated with the atmospheric aerosol are proportional to HNO_2 concentrations in the gas-phase according to the Henry's Law. Therefore, here we use aerosol NO_2^- as an indicator for primary vehicular emissions. From the very low correlation coefficients between oxalate and NO_2^- in every season ($r = 0.07$ – 0.25), we concluded that the vehicular emission made a very limited contribution to the total amount of aerosol oxalate in Shanghai as a primary source. Hence, the secondary formation in the atmosphere should account for the majority of this compound.

A high correlation was found between oxalate and NO_3^- ($r = 0.49$ – 0.90) in $PM_{2.5}$, suggesting a similar source or formation pathway between these two species. The atmospheric precursors of NO_3^- and oxalate were NO_x and

Table 5 The correlation coefficients between oxalate and several source-indicating species in PM_{2.5} in Shanghai, 2007

	Sample numbers	Al	NO ₂ ⁻	NO ₃ ⁻	nss-SO ₄ ²⁻ ^c	NH ₄ ⁺	K ⁺
Spring	34	0.53 ^a	0.19	0.80 ^a	0.85 ^a	0.60 ^a	0.53 ^a
Summer	28	0.36 ^b	0.21	0.90 ^a	0.95 ^a	0.80 ^a	0.51 ^a
Autumn	27	0.02	0.25 ^b	0.49 ^a	0.60 ^a	0.52 ^a	0.65 ^a
Winter	31	0.10	0.07	0.60 ^a	0.67 ^a	0.59 ^a	0.29 ^b

^a Correlation is significant at $P < 0.01$ level

^b Correlation is significant at $P < 0.05$ level

^c Non-sea salt sulfate

volatile organic matters (e.g., alkenes) respectively, a characteristic source of which in urban city was vehicular exhausts. The good correlation between aerosol NO₃⁻ and oxalate provided evidence that vehicular emission was a major secondary source for these two compounds in Shanghai. Furthermore, the conversion of NO₂ to NO₃⁻, which is activated by ozone or radicals like OH and the formation of oxalate from alkenes which was also supposed to be a radical involved oxidation process, could be parallel and internally linked to each other through gaseous or aqueous radicals. For oxalate resided in particle size range larger than droplet mode (>1.0 μm), it could be produced by surface reactions of gaseous oxalic acid or its precursors with alkaline coarse particles or from the evaporation of oxalate in smaller size range [11, 30]. These could be two possible formation pathways for oxalate in higher fine particle mode (1.0–2.5 μm). However, more nitric acid was evaporated from fine particles and absorbed by alkaline coarse particles compared to oxalic acid due to their different volatility. This provided a reasonable explanation for the high correlation and distinct-size distribution between these two compounds.

As a result of a number of the previous studies, the formation of sulfate in the atmosphere through aqueous-phase oxidation is well established. Some researchers concluded from simulations that in-cloud process could convert up to 80 % SO₂ to sulfate in troposphere [40]. Recent studies evidenced that the secondary formation of oxalate in the troposphere also requires the aqueous medium, with glyoxylate as a key aqueous-phase precursor [12, 20]. In Shanghai, aerosol oxalate showed a strong correlation with nss-sulfate in all four seasons ($r = 0.60$ – 0.95), especially in summer ($r = 0.95$), suggesting a common formation pathway between these two species. The similarity in oxalate and sulfate's distribution between PM_{2.5} and TSP also offered support to this hypothesis. As mentioned in the size distribution analysis and a number of studies, aerosol oxalate and sulfate mainly resided in fine particles and both probably represented a dominant droplet particle mode (<1.0 μm). Based on plenty of previous

studies, aqueous-phase reactions were necessary to the production of droplet mode sulfate as well as that of droplet mode secondary aerosol organics to occur [16]. That is to say, the cloud process was suggested to be the most possible common formation pathway of aerosol oxalate and sulfate, considering the particle-size distribution.

Ammonium also showed an obvious positive correlation with oxalate, with the correlation coefficients of 0.52–0.80. One possible explanation of this phenomenon is that ammonium in the atmosphere is mainly produced by the reaction between gaseous NH₃ and acidic sulfate particles [41] and therefore its high correlation with oxalate might be affected (or brought) by sulfate. On the other hand, it could be explained by the presence of ammonium oxalate in aerosols. Lefer and Talbot [42] suggested that ammonium oxalate aerosol may be directly formed from the gaseous ammonia and oxalic acid. Combined with the result of size distribution analysis, the high correlation between ammonium and oxalate indicated a possible form of existence for aerosol oxalate rather than evidence for a common source.

Since K⁺ is an essential nutrient element for the growth of plants, it has been used as an effective indicator for the source of atmospheric particulates from biomass burning, especially in the fine particle mode [14, 32, 43]. The size distribution characteristics of K⁺ observed in this work also showed that K⁺ dominantly resides in PM_{2.5} in every season in urban Shanghai (~80 %). The results of correlation analysis presented a moderate correlation between oxalate and K⁺ with a peak value in autumn ($r = 0.65$), being consistent with the fact that the events of biomass burning happened most frequently in this season. If an oxalate/K⁺ correlation suggested the contribution of biomass burning to the aerosol oxalate concentrations, there is a question needed to be addressed: is biomass burning just a primary source or also a secondary source for aerosol oxalate since biogenic VOCs could be released to the atmosphere through the biomass burning activity? The ratio of oxalate to K⁺ (oxalate/K⁺) in this work averaged at 0.26 in autumn, which was apparently larger than the reported values for the oxalate directly measured in biomass burning plumes (0.03–0.1) [43]. On the other hand, the high content of water-soluble compounds (inorganic salts and water-soluble organic matters) in biomass burning aerosols made the majority of them act as CCN [44, 45]. Hence, the high oxalate/K⁺ ratio suggested a secondary formation of oxalate from biomass burning emitted VOCs and probably through an in-cloud pathway as well. This is exactly the reason that VOCs precursors of oxalate had a characteristic source from biomass burning in autumn that could partially explain the observation of the highest oxalate concentration and the lowest correlation coefficient between oxalate, nitrate, and sulfate in this season.

3.2.2 Linear relationship of oxalate with sulfate/nitrate

The relationships of aerosol oxalate with the two source-indicating species, nss-SO_4^{2-} and NO_3^- , could give a hint to the secondary formation pathways of aerosol oxalate. As mentioned above, the oxidation of SO_2 to SO_4^{2-} in the atmosphere mainly happens in the aqueous phase, where the dissolved SO_2 forms HSO_3^- and SO_3^{2-} and then oxidized by ozone or hydroperoxides at significant rates. Meanwhile, aqueous-phase formation was regarded as necessary for the production of droplet mode secondary organic aerosol to occur [16], which was applicable to the majority of aerosol oxalate in Shanghai based on previous discussions. Differently, the oxidation of NO_2 to nitric acid in the atmosphere mostly occurs in the gaseous phase, either oxidized by OH radical directly or by ozone through two intermediates, NO_3 radical and nitrogen pentoxide [46]. Previous studies [12, 21, 47] suggested that atmospheric oxalate is dominantly produced through aqueous oxidation by OH radical with glyoxylic acid, the most immediate precursor, which derived from either gaseous or aqueous oxidation of various primary precursors, ethene, acetylene, isoprene from biogenic source, etc. It was noticed that OH radical was involved in secondary formations of both NO_3^- and oxalate in the atmosphere. That is to say, the productions of NO_3^- and oxalate would be limited by the availability of OH radical. From this point of view, the secondary formations of these two species were internally related.

Looking at our data, summer and winter as representative seasons, the sulfate-oxalate and nitrate-oxalate correlation coefficients were better in summer (0.95 and 0.90) than in winter (0.67 and 0.60) (Table 5). Furthermore, the slope values of sulfate-oxalate and nitrate-oxalate linear regression curves were both lower in summer than in winter (Fig. 3a, b). Seasonal characteristics of these three compounds may explain the difference. As discussed before, sulfate, nitrate, and oxalate in fine particles were mainly secondarily formed in the atmosphere of Shanghai and probably through related formation pathways. In summer, local sources of the three compounds were predominant which made the correlations between them significant. In winter, with the invading northwesterly from the continent, sulfate, nitrate, and oxalate from sources out-of-Shanghai would be brought to the local atmosphere and hence decrease their correlations to each other. On the other hand, ambient concentrations of SO_2 and NO_2 were lifted in winter owing to the bad atmospheric diffusion in this season (Table 1). Meanwhile, emission of VOCs was lessened under the low temperature of winter. Consequently, differences in concentrations of sulfate and nitrate and that of aerosol oxalate (the slope values) were widened.

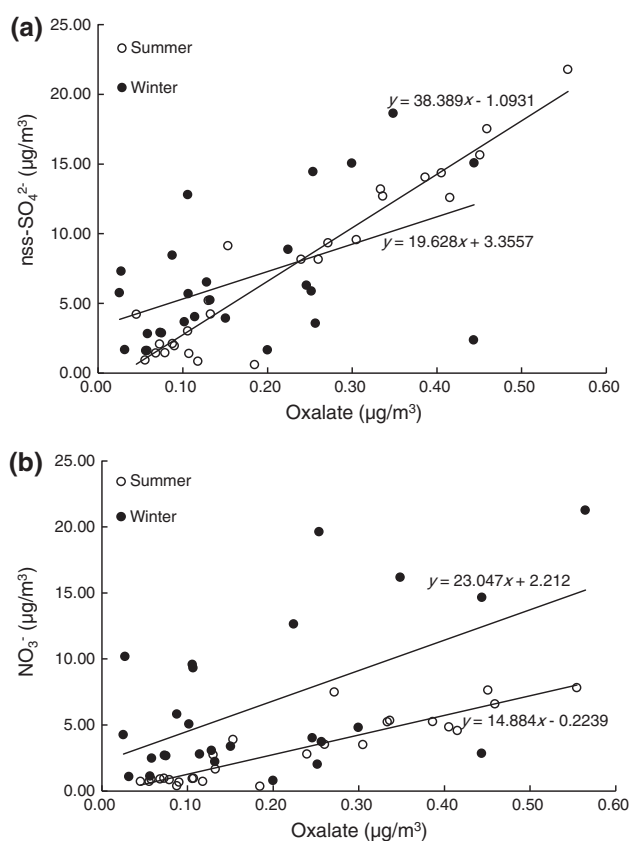


Fig. 3 The linear regression curves of oxalate- nss-SO_4^{2-} (a) and oxalate- NO_3^- (b) in $\text{PM}_{2.5}$ in summer and winter

3.2.3 Meteorological evidence for the formation pathway of aerosol oxalate

Meteorological factors were taken into account for the formation of aerosol oxalate in Shanghai. The variation of temperature, relative humidity (RH), cloud cover, wind speed (WS), and wind direction (WD) in the sampling period were compared with that of the oxalate concentrations. Based on the daily average observation values, no significant quantitative correlation was found between oxalate and any of these meteorological factors. However, the oxalate concentration did increase under such weather conditions: (1) clear days with clouds; (2) days with haze, mist or fog; and (3) rain or shower or thunderstorm happening in the sampling days. Should the concentration level of aerosol oxalate be simultaneously influenced by multiple meteorological parameters? The time series of relative humidity (RH), cloud cover and oxalate concentration through the sampling period are shown in Fig. 4. It could be concluded from the temporal trends that whenever both the relative humidity and cloud cover declined compared to the values in the preceding day, a decrease of oxalate concentration was observed accordingly and vice versa (see the dash lines in gray in Fig. 4). That is to say,

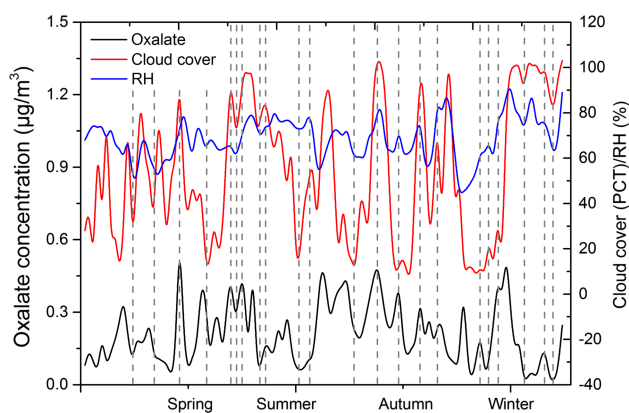


Fig. 4 Time series of oxalate concentration, relative humidity (RH) and cloud cover through the sampling period

simultaneous increases in ambient RH and cloud cover would indicate the rise in oxalate concentration in the same days.

The influence brought by the variations of meteorological conditions and the differences between the sources and concentration levels of VOCs precursors of oxalate in such a time scale could be reduced to a large extent by comparing the data of every two neighboring days. These two positive contributing meteorological factors to the ambient concentration of the compound implied that a secondary formation of aerosol oxalate in aqueous medium did exist in Shanghai and probably through an in-cloud pathway.

3.3 Aerosol oxalate and haze pollution

One of the meteorological factors, visibility, was selected for the further study on aerosol oxalate due to its strong relationship with haze pollution. Haze is defined as the weather phenomenon which leads to atmospheric visibility less than 10 km due to the moisture, dust, smoke, and vapor in the atmosphere. Haze pollution has drawn great attention in the past decade for its impact on visibility, public health, and even climate change [48–50]. The characteristics and formation mechanism of haze may vary in different regions. However, many studies on haze pollution, including study in Shanghai and its surrounding areas indicated that high mass fractions of water-soluble inorganic ions, such as NH_4^+ , SO_4^{2-} , and NO_3^- in $\text{PM}_{2.5}$ were observed during the haze episodes [29, 51, 52]. Haze episodes had such a characteristic of increased mass fractions of certain hygroscopic species, suggesting that contribution of these hygroscopic species to the degradation of visibility was greater than that of other species in the aerosols. As a water-soluble organic compound (WSOC), the role of oxalate in haze formation was investigated by comparing the variation of oxalate concentration and daily visibility of Shanghai in four seasons. As shown in Fig. 5,

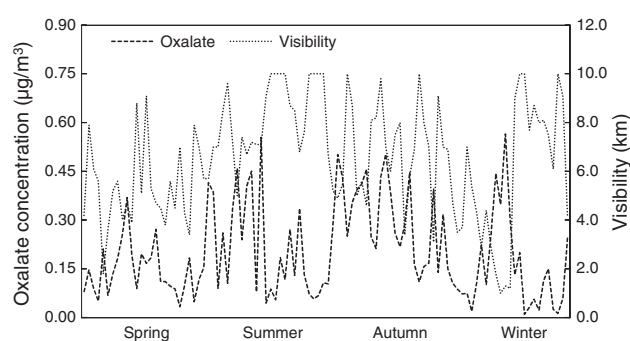


Fig. 5 Variations of oxalate concentrations in $\text{PM}_{2.5}$ and visibilities in four seasons of Shanghai

visibility of the city showed a strong-negative correlation with the oxalate concentration levels in each season. The correlation coefficient r between visibility and oxalate concentration was -0.32 in average and -0.42 at peak value.

In general, aerosol oxalate comprises less than 1 % of the aerosol mass as a water-soluble organic compound. The oxalate–WSOC–aerosol OC–aerosol mass relationship was first examined to illustrate what the negative correlation between oxalate concentration and atmospheric visibility implied. WSOC usually accounted for 20 %–70 % of aerosol OC [53, 54]. This percentage would be near the high end of the range in large urban center as Shanghai where more hygroscopic secondary organic aerosol (SOA) comprised a large fraction of ambient aerosol OC, due to the increase in polarity that accompanies the oxidizing formation pathway of SOA [55, 56]. Without direct measurement, the OC content of the aerosol was estimated by the concentrations of ions, elements, and black carbon (BC). The method of the calculation was shown below [57]: (1) crust = $\text{Al}/0.08$; (2) secondary = $\text{NH}_4^+ + \text{NO}_3^- + \text{SO}_4^{2-}$; (3) sea salt = $2.54 \times (\text{Na} - 0.3\text{Al})$; (4) smoke = $\text{K} - 0.25\text{Al}$; (5) metals = the sum of the mass of all detected non-crustal/non-sea salt elements by ICP-AES; (6) aerosol carbonaceous species, roughly estimated with a mass balance, neglecting those minor components and H_2O , = aerosol mass – sum of ((1)–(5)); and (7) $\text{OC} \times 1.8 = \text{carbonaceous species} - \text{EC}$, here BC was used to represent EC for a rough estimate [58]. The relative contributions of OC and major inorganic salts in $\text{PM}_{2.5}$ in Shanghai, 2007 are shown in Fig. 6. Organic carbon was estimated contributing over 30 % of the total $\text{PM}_{2.5}$ mass concentration in average, which was consistent with results of studies [59] carried out in a worldwide range suggesting that $\sim 20\%$ – 80% of fine particle mass was organic. Comparably, the sum of the mass concentrations of SO_4^{2-} , NO_3^- , NH_4^+ , and K^+ took $\sim 20\%$ of that of the total $\text{PM}_{2.5}$. If the OM (organic matter)/OC ratio of 1.8 and WSOC/OC ratio of 50 % was applied in this study,

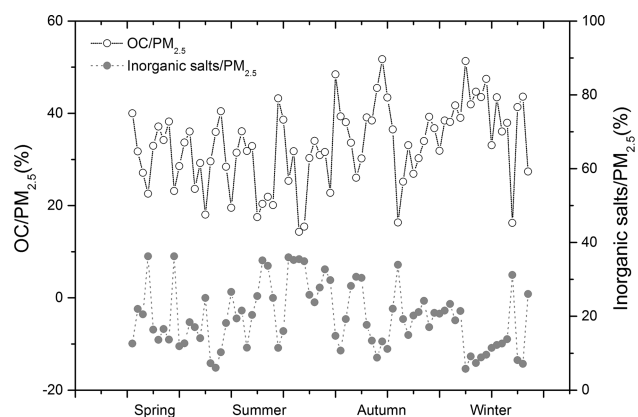


Fig. 6 Relative contributions of OC (estimated) and major inorganic salts (observed, SO_4^{2-} , NO_3^- , NH_4^+ , and K^+) in $\text{PM}_{2.5}$ in Shanghai, 2007

averagely 27 % of the $\text{PM}_{2.5}$ mass concentration would be occupied by water-soluble organic compounds, which was larger than the portion those major inorganic salts took.

The existence of WSOC in aerosol would make the aerosol more hygroscopic and thus easier to act as condensation nuclei. Being the most abundant identified dicarboxylic acid in the tropospheric aerosol and a water-soluble compound, oxalate could be taken as a representative compound of the WSOC in the aerosols. The rise of aerosol oxalate concentration in the atmosphere reflected the rise of WSOC content to a certain extent, which would be more favorable to the formation of haze. On the other hand, studies [60, 61] found that in areas where the portion of OC in atmospheric aerosol is significant and the ambient RH is high, the change of extinction coefficient due to water uptake by the aerosol organic compounds is an important factor influencing the aerosol optical properties. Aerosol organic compounds were proved to be able to scatter similar solar radiation as sulfate aerosol did. And these changes in aerosol extinction coefficient arisen from the organic fraction were not dependent on either the concentration or the specific composition of it. Research carried out in south China also reported that the extinction and scattering efficiencies (α_{ep} , α_{sp}) of aerosol organic matter were rather high and close to those of aerosol sulfate and nitrate [62]. Observation at Fudan University sampling site in early spring 2009 (January 15 to February 4) confirmed that organic matter (OM), sulfate and nitrate were the main light scattering components in aerosols which accounted for 50.6 %, 23.8 %, and 15.1 % of the light the aerosol scattered, respectively [63]. Such high content and extinction efficiency made aerosol organic compounds the key components contributing to the degradation of atmospheric visibility in Shanghai. Furthermore, some of the water-insoluble organics in aerosols can interact with certain water-soluble inorganic compounds, such as SO_4^{2-} , to form

an organic–inorganic complex and promote efficient new formation of both parties in aerosols [64]. Therefore, the distinct negative correlation of atmospheric visibility with aerosol oxalate concentration, together with the high percentage of WSOC and/or OC in the aerosols in Shanghai implied that aerosol organic compounds played an important role in the formation of haze as well as in shaping the characteristics of atmospheric aerosol in megacities.

4 Conclusions

The mass concentrations of oxalate in 2007 sampling year were $0.07\text{--}0.41 \mu\text{g}/\text{m}^3$ in $\text{PM}_{2.5}$ and $0.10\text{--}0.48 \mu\text{g}/\text{m}^3$ in TSP, respectively. The oxalate concentrations displayed a seasonal variation of autumn > summer > winter > spring in both particle modes. Oxalate was dominantly present in $\text{PM}_{2.5}$ or even finer particle mode ($<1.0 \mu\text{m}$) in all samples, and the peak value of $\text{PM}_{2.5}/\text{TSP}$ appeared in summer. Nss-SO_4^{2-} , NH_4^+ and K^+ showed a dominant residence in $\text{PM}_{2.5}$ as oxalate did while NO_3^- had obviously lower values of $\text{PM}_{2.5}/\text{TSP}$ in all four seasons. In a recorded dust day, it was observed that invading dust brought gaseous or particulate oxalate to Shanghai as well as made local oxalate partitioning more to the coarse particle mode. As a result, a sharply increased oxalate level and decreased $\text{PM}_{2.5}/\text{TSP}$ ratio of oxalate concentration was obtained during the dust episode.

Based on the correlation analysis between aerosol oxalate and source-indicating species, crustal source and vehicular emission was found minor contributors to the total amount of oxalate as primary sources. Considering the good correlation between oxalate and K^+ and high ratio of oxalate/ K^+ , biomass burning was proved to be a secondary source of aerosol oxalate in Shanghai, in addition to urban VOCs sources (vehicular and industrial emissions), especially in autumn. Secondary formation accounted for the majority of aerosol oxalate in each season of Shanghai and mainly took place through an aqueous-phase oxidation pathway as aerosol SO_4^{2-} did. This conclusion was supported by the high correlation of oxalate with nss-SO_4^{2-} and K^+ , dominant residence of oxalate in droplet mode and result of favorable meteorological condition analysis, in which high oxalate concentration was observed when relatively high ambient RH and high cloud cover happened simultaneously. However, since gaseous-phase oxidations happened in the early stages of the production of oxalate from alkenes in the atmosphere, the high correlation of oxalate and NO_3^- suggested that the formation of these two compounds was internally linked through the radicals involved. Due to the large fraction of WSOC in $\text{PM}_{2.5}$ in Shanghai, oxalate as representative compound of it, its contribution to the haze pollution and visibility degradation

of the local environment was comparable to that of the water-soluble inorganic species in the aerosols. The role of oxalate together with other aerosol organic compounds in the haze pollution and urban air quality needs to be further studied.

Acknowledgments This study was supported by the Great International Collaboration Project of MOST, China (2010DFA92230), the National Basic Research Program of China (2006CB403704), and the National Natural Science Foundation of China (20877020 and 20977017).

References

- Kawamura K, Ikushima K (1993) Seasonal changes in the distribution of dicarboxylic acids in the urban atmosphere. *Environ Sci Technol* 27:2227–2235
- Facchini MC, Fuzzi S, Zappoli S et al (1999) Partitioning of the organic aerosol component between fog droplets and interstitial air. *J Geophys Res* 104:26821–26832
- Mader BT, Yu JZ, Xu JH et al (2004) Molecular composition of the water-soluble fraction of atmospheric carbonaceous aerosols collected during ACE: Asia. *J Geophys Res* 109:D06206. doi:10.1029/2003JD004105
- Cruz CN, Pandis SN (1998) The effect of organic coatings on the cloud condensation nuclei activation of inorganic atmospheric aerosol. *J Geophys Res* 103:13111–13123
- Kumar PP, Broekhuizen K, Abbatt JPD (2003) Organic acids as cloud condensation nuclei: laboratory studies of highly soluble and insoluble species. *Atmos Chem Phys* 3:509–520
- Facchini MC, Mircea M, Fuzzi S et al (1999) Cloud albedo enhancement by surface-active organic solutes in growing droplets. *Nature* 401:257–259
- Kerminen VM (2001) Relative roles of secondary sulfate and organics in atmospheric cloud condensation nuclei production. *J Geophys Res* 106:17321–17333
- Lu GX, Guo XL (2012) Distribution and origin of aerosol and its transform relationship with CCN derived from the spring multi-aircraft measurements of Beijing cloud experiment (BCE). *Chin Sci Bull* 57:2460–2469
- Jickells TD, An ZS, Andersen KK et al (2005) Global iron connections between desert dust, ocean biogeochemistry, and climate. *Science* 308:67–71
- Kawamura K, Sakaguchi F (1999) Molecular distributions of water soluble dicarboxylic acids in marine aerosols over the Pacific Ocean including tropics. *J Geophys Res* 104:3501–3509
- Kerminen VM, Ojanen C, Pakkanen T et al (2000) Low-molecular weight dicarboxylic acids in an urban and rural atmosphere. *J Aerosol Sci* 31:349–362
- Carlton AG, Turpin BJ, Altieri KE et al (2007) Atmospheric oxalic acid and SOA production from glyoxal: results of aqueous photooxidation experiments. *Atmos Environ* 41:7588–7602
- Sullivan RC, Prather KA (2007) Investigations of the diurnal cycle and mixing state of oxalic acid in individual particles in Asian aerosol outflow. *Environ Sci Technol* 41:8062–8069
- Huang XF, Yu JZ, He LY et al (2006) Water-soluble organic carbon and oxalate in aerosols at a coastal urban site in China: size distribution characteristics, sources, and formation mechanism. *J Geophys Res* 111:D22212. doi:10.1029/2006JD007408
- Seinfeld JH, Pandis SN (1998) *Atmospheric chemistry and physics: from air pollution to climate change*. Wiley-Interscience, New York
- Blando JD, Turpin BJ (2000) Secondary organic aerosol formation in cloud and fog droplets: a literature evaluation of plausibility. *Atmos Environ* 34:1623–1632
- Yao XH, Lau APS, Fang M et al (2003) Size distribution and formation of ionic species in atmospheric particulate pollutants in Beijing, China: 2-dicarboxylic acids. *Atmos Environ* 37:3001–3007
- Crahan KK, Hegg D, Covert DS et al (2004) An exploration of aqueous oxalic acid production in the coastal marine atmosphere. *Atmos Environ* 38:3757–3764
- Yu JZ, Huang XF, Xu J et al (2005) When aerosol sulfate goes up, so does oxalate: implication for the formation mechanisms of oxalate. *Environ Sci Technol* 39:128–133
- Sorooshian A, Varutbangkul V, Brechtel FJ et al (2006) Oxalic acid in clear and cloudy atmospheres: analysis of data from international consortium for atmospheric research on transport and transformation 2004. *J Geophys Res* 111:D23S45. doi:10.1029/2005JD006880
- Martinello PK, Dasgupta PK, Al-Horr RS (2007) Atmospheric production of oxalic acid/oxalate and nitric acid/nitrate in the Tampa Bay airshed: parallel pathways. *Atmos Environ* 41:4258–4269
- Yin J, Tan J (2003) Effect of surface wind direction on air pollutant concentrations in Shanghai. *Meteorol Sci Technol* 31:366–369 (in Chinese)
- Taha G, Box GP, Cohen DD et al (2007) Black carbon measurement using laser integrating plate method. *Aerosol Sci Technol* 41:266–276
- Yuan H, Wang Y, Zhuang GS (2003) Simultaneous determination of organic acids, methane sulfonic acid and inorganic anions in aerosol and precipitation samples by ion chromatography. *J Instrum Anal* 22:11–14 (in Chinese)
- Zhuang G, Guo JH, Yuan H et al (2001) The compositions, sources, and size distribution of the dust storm from China in spring of 2000 and its impact on the global environment. *Chin Sci Bull* 46:895–901
- Sun YL, Zhuang GS, Wang Y et al (2004) The air-borne particulate pollution at Beijing—concentrations, composition, distribution, and sources of Beijing aerosol. *Atmos Environ* 38:5991–6004
- Limbeck A, Puxbaum H, Otter L et al (2001) Semivolatile behavior of dicarboxylic acids and other polar organic species at a rural background site (Nylsvley, RSA). *Atmos Environ* 35:1853–1862
- Pathak RK, Chan CK (2005) Inter-particle and gas-particle interactions in sampling artifacts of PM_{2.5} in filter-based samplers. *Atmos Environ* 39:1597–1607
- Fu QY, Zhuang GS, Wang J et al (2008) Mechanism of formation of the heaviest pollution episode ever recorded in the Yangtze River Delta, China. *Atmos Environ* 42:2023–2036
- Yao XH, Chan CK, Fang M et al (2002) The water-soluble ionic composition of PM_{2.5} in Shanghai and Beijing, China. *Atmos Environ* 36:4223–4234
- Yang H, Yu JZ, Ho SS et al (2005) The chemical composition of inorganic and carbonaceous materials in PM_{2.5} in Nanjing, China. *Atmos Environ* 39:3735–3749
- Yao XH, Fang M, Chan CK et al (2004) Characterization of dicarboxylic acids in PM_{2.5} in Hong Kong. *Atmos Environ* 38:963–970
- Wang Y, Zhuang GS, Chen S et al (2007) Characteristics and sources of formic, acetic and oxalic acids in PM_{2.5} and PM₁₀ in Beijing, China. *Atmos Res* 84:169–181
- Sempere R, Kawamura K (1994) Comparative distribution of dicarboxylic acids and related polar compounds in snow, rain and aerosols from urban atmosphere. *Atmos Environ* 28:449–459

35. Uchiyama S (1996) The behavior of oxalic acid in atmospheric aerosols. *Jpn Soc Atmos Environ* 31:141–148
36. Kawamura K, Kaplan IR (1987) Motor exhaust emissions as a primary source for dicarboxylic acids in Los Angeles ambient air. *Environ Sci Technol* 21:105–110
37. Dasgupta PK, Campbell SW, Al-Horr RS et al (2007) Conversion of sea salt aerosol to and the production of HCl: analysis of temporal behavior of aerosol chloride/nitrate and gaseous HCl/HNO₃ concentrations with AIM. *Atmos Environ* 41:4242–4257
38. Zhuang H, Chan CK, Fang M et al (1999) Size distributions of particulate sulfate, nitrate, and ammonium at a coastal site in Hong Kong. *Atmos Environ* 33:843–853
39. Pitts JN Jr, Biermann HW, Winer AM et al (1984) Spectroscopic identification and measurement of gaseous nitrous acid in dilute auto exhaust. *Atmos Environ* 18:847–854
40. McHenry JN, Dennis RL (1994) The relative importance of oxidation pathways and clouds to atmospheric ambient sulfate production as predicted by the regional acid deposition model. *J Appl Meteorol Clim* 33:890–905
41. Finlayson-Pitts BJ, Pitts JN Jr (1999) Chemistry of the upper and lower atmosphere: theory, experiments, and applications. Academic Press, New York
42. Lefer BL, Talbot RW (2001) Summertime measurements of aerosol nitrate and ammonium at northeastern U.S. site. *J Geophys Res* 106:20365–20378
43. Yamasoe MA, Artaxo P, Miguel AH et al (2000) Chemical composition of aerosol particles from direct emissions of vegetation fires in the Amazon Basin: water soluble species and trace elements. *Atmos Environ* 34:1641–1653
44. Rogers CF, Hudson GJ, Zielinska B et al (1991) Global biomass burning: atmospheric, climatic and biospheric implications. MIT Press, Cambridge, MA
45. Novakov T, Corrigan CE (1996) Cloud condensation nucleus activity of the organic component of biomass smoke particles. *Geophys Res Lett* 23:2141–2144
46. Warneck P (1999) Chemistry of the natural atmosphere. Academic Press, London
47. Warneck P (2003) In-cloud chemistry opens pathway to the formation of oxalic acid in the marine atmosphere. *Atmos Environ* 37:2423–2427
48. Okada K, Ikegami M, Zaizen Y et al (2001) The mixture state of individual aerosol particles in the 1997 Indonesian haze episode. *J Aerosol Sci* 32:1269–1279
49. Chen LWA, Chow JC, Doddridge BG et al (2003) Analysis of a summertime PM_{2.5} and haze episode in the mid-Atlantic region. *J Air Waste Manage Assoc* 53:946–956
50. Yadav AK, Kumar K, Kasim A et al (2003) Visibility and incidence of respiratory diseases during the 1998 haze episode in Brunei Darussalam. *Pure Appl Geophys* 160:265–277
51. Sun YL, Zhuang GS, Tang AH et al (2006) Chemical characteristics of PM_{2.5} and PM₁₀ in haze-fog episodes in Beijing. *Environ Sci Technol* 41:3148–3155
52. An JL, Li Y, Chen Y et al (2013) Enhancements of major aerosol components due to additional HONO sources in the North China Plain and implications for visibility and haze. *Adv Atmos Sci* 30:57–66
53. Decesari S, Facchini MC, Matta E et al (2001) Chemical features and seasonal variation of water soluble organic compounds in the Po valley fine aerosol. *Atmos Environ* 35:3691–3699
54. Decesari S, Fuzzi S, Facchini MC et al (2006) Characterization of the organic composition of aerosols from Rondonia, Brazil, during the LBA-SMOCC 2002 experiment and its representation through model compounds. *Atmos Chem Phys* 6:375–402
55. Lim HJ, Turpin BJ (2002) Origins of primary and secondary organic aerosol in Atlanta: results of time-resolved measurements during the Atlanta supersite experiment. *Environ Sci Technol* 36:4489–4496
56. Hennigan CJ, Bergin MH, Weber RJ (2008) Correlations between water-soluble organic aerosol and water vapor: a synergistic effect from biogenic emissions. *Environ Sci Technol* 42:9079–9085
57. Wang Y, Zhuang GS, Tang AH et al (2007) The evolution of chemical components of aerosols at five monitoring sites of China during dust storms. *Atmos Environ* 41:1091–1106
58. Chow JC, Watson JG, Doraiswamy P et al (2009) Aerosol light absorption, black carbon, and elemental carbon at the Fresno Supersite, California. *Atmos Res* 93:874–887
59. Zhang Q, Jimenez J (2007) Ubiquity and dominance of oxygenated species in organic aerosols in anthropogenically-influenced Northern Hemisphere midlatitudes. *Geophys Res Lett* 34:L13801. doi:10.1029/2007GL029979
60. Myhre CEL, Nielson CJ (2004) Optical properties in the UV and visible spectral region of organic acids relevant to tropospheric aerosols. *Atmos Chem Phys* 4:1759–1769
61. Garland RM, Ravishankara AR, Lovejoy ER et al (2007) Parameterization for the relative humidity dependence of light extinction: organic-ammonium sulfate aerosol. *J Geophys Res* 112:D19303. doi:10.1029/2006JD008179
62. Cheng Y, Wiedensohler A, Eichler H et al (2008) Aerosol optical properties and related chemical apportionment at Xinken in Pearl River Delta of China. *Atmos Environ* 42:6351–6372
63. Huang K (2010) The transformation of aerosol components during the long-range transport of Asian dust and the formation mechanism of haze in mega-city, China. Dissertation, Fudan University (in Chinese)
64. Zhang RY, Suh I, Zhao J et al (2004) Atmospheric new particle formation enhanced by organic acids. *Science* 304:1487–1490



Chinese Science Bulletin
Volume 56, Number 1, January 2013
ISSN 02-1226, CN 11-1706

Special Topic: Spectral Analysis
Four-level active optical clock
Scriptaid enhances pig epigenetic reprogramming
Short term climatic impacts of afforestation
The role of acyl chain energy

Effects of lactic acid on stem cells
Superconducting coolant waveguide resonator
Acoustic optical properties
KTP impurities in parosia and fatty liver
Cosmogenic ¹⁰Be denudation rates of carbonates

SPECIAL ISSUE
Extreme Climate in China

More Oriental features
Valid boundary between
Structure change of PTT containing
ATHK1 regulates calcium channel
Photothermal- and laser-
Cell proliferation promoted
two *SIRT6* variants
Stable isotopes in Antarctic snow
New terpenoids from *Zieria cur*
Superconducting nanowire single-
Structure variations in a superlattice

Chinese Science Bulletin
Volume 56, Number 2, February 2013
ISSN 02-1226, CN 11-1706

Genome analysis of the caterpillar *Tringia*
ESG tags protect against renal ischemia
Chinese exerts in LGM and HoloBorneo
Blood incompatibility of Mg-Nd-Zn alloy

Electrostatic analysis of the face-to-face dimer interface
PCDD/Fs and PCBs in Tianjin air
A reduced chemical kinetic model
Small-influenced temperature changes on Tibetan Plateau

Alveolar remodeling in Jurassic *Tyrannosaurus*
The asymmetry of rainfall process
Origin of *H. pylori* in humans infection
Electron transfer in molten ionic liquids
Subcellular Proteomics: gaselle

Chinese Science Bulletin
Volume 56, Number 3, March 2013
ISSN 02-1226, CN 11-1706

Chinese Science Bulletin
Volume 56, Number 4, April 2013
ISSN 02-1226, CN 11-1706

Emotion regulation explored by ERP
Albino spin gyrospace based on "No-Be"
Polymer single nanochannels: a biosensor
TmSd₂XO₂ oligo film synthesized by GDSAT
Flow pattern modulation in tube

Chinese Science Bulletin
2013 Cover Gallery
Submit Your Cover Images to CSB

ARK methods for gaseous detonation simulation
Branched chain amino acids and metabolic regulation
Ionic liquids for synthesis of polyarylether ketone
Observation of thermosensitive liquid
Ultracompact in Ga₂ crystals

Chinese Science Bulletin
Volume 56, Number 5, May 2013
ISSN 02-1226, CN 11-1706

Chinese Science Bulletin
Volume 56, Number 6, June 2013
ISSN 02-1226, CN 11-1706

Isolation of a novel brittle culm gene
Biopromoting quantum dot for enzyme detection
Applicability of transposon SHM method
Modeling of static sea level

DNMTs and chromosomes in oocytes of aging mice
Construction of a bacterial artificial chromosome library
Its promote aromatic acid esterification
A multi-model approach for research evaluation

Biosorption and biodegradation of PAHs
Pre-orbital determination of Hepatitis B
Bird distribution changes in China
Estimating organic carbon in China's wetlands
Microbial ammonia nitrogen fixation in soil

Change of biodiversity patterns in coastal zone
Quaternary relation algorithm
Pollutants degradation by a Co₂O
First therapeutic stem cell pathway from
Tumor targeting therapeutics

Chinese Science Bulletin
Volume 56, Number 7, July 2013
ISSN 02-1226, CN 11-1706

Mesless method for disc

Chinese Science Bulletin
Volume 56, Number 8, August 2013
ISSN 02-1226, CN 11-1706

Chinese Science Bulletin
Volume 56, Number 9, September 2013
ISSN 02-1226, CN 11-1706

Chinese Science Bulletin
Volume 56, Number 10, October 2013
ISSN 02-1226, CN 11-1706

Chinese Science Bulletin
Volume 56, Number 11, November 2013
ISSN 02-1226, CN 11-1706

Chinese Science Bulletin
Volume 56, Number 12, December 2013
ISSN 02-1226, CN 11-1706

Chinese Science Bulletin
Volume 56, Number 1, January 2014
ISSN 02-1226, CN 11-1706

Chinese Science Bulletin
Volume 56, Number 2, February 2014
ISSN 02-1226, CN 11-1706

Chinese Science Bulletin
Volume 56, Number 3, March 2014
ISSN 02-1226, CN 11-1706

Chinese Science Bulletin
Volume 56, Number 4, April 2014
ISSN 02-1226, CN 11-1706

Chinese Science Bulletin
Volume 56, Number 5, May 2014
ISSN 02-1226, CN 11-1706

Chinese Science Bulletin
Volume 56, Number 6, June 2014
ISSN 02-1226, CN 11-1706

Chinese Science Bulletin
Volume 56, Number 7, July 2014
ISSN 02-1226, CN 11-1706

Chinese Science Bulletin
Volume 56, Number 8, August 2014
ISSN 02-1226, CN 11-1706

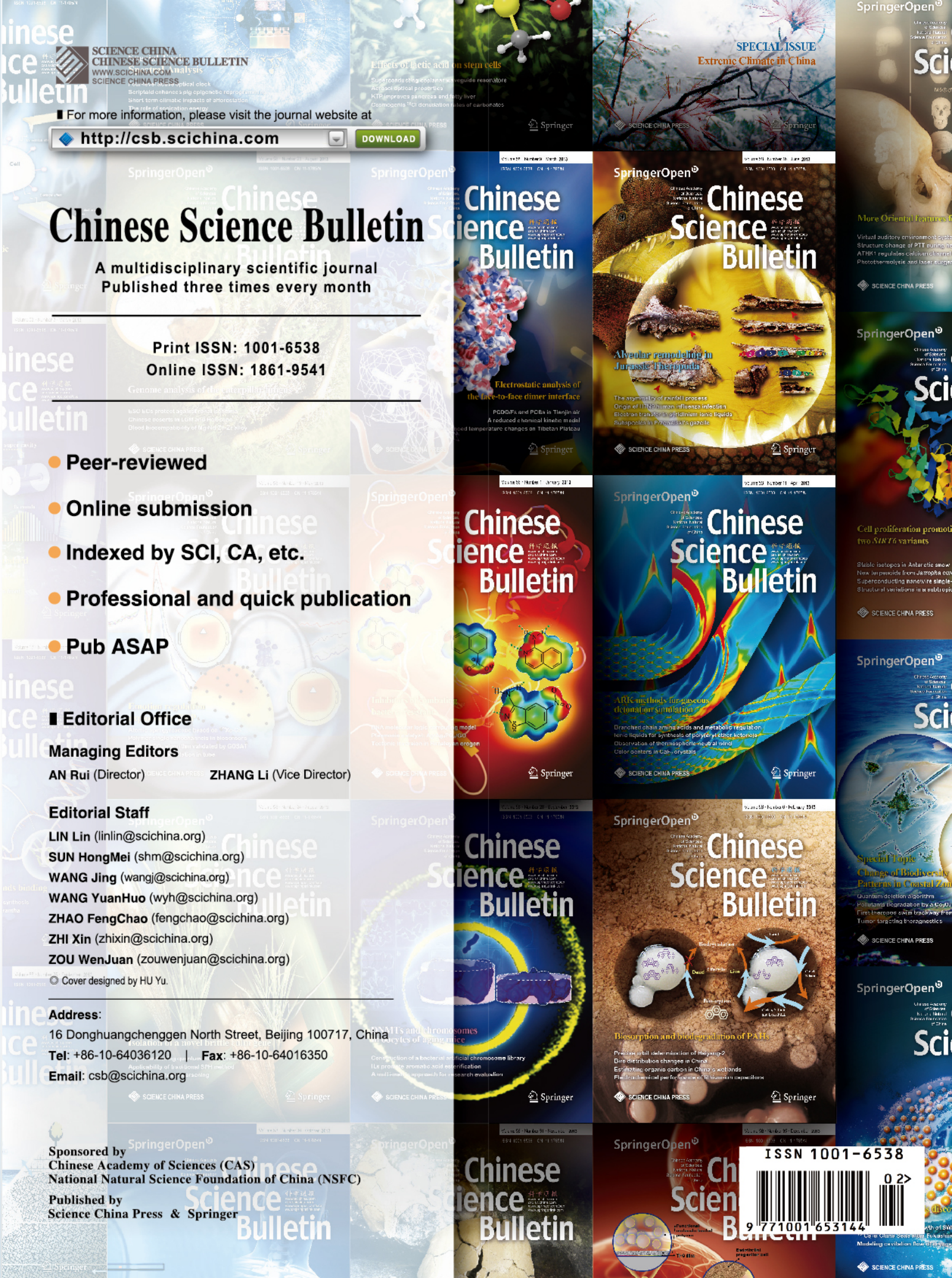
Chinese Science Bulletin
Volume 56, Number 9, September 2014
ISSN 02-1226, CN 11-1706

Chinese Science Bulletin
Volume 56, Number 10, October 2014
ISSN 02-1226, CN 11-1706

Chinese Science Bulletin
Volume 56, Number 11, November 2014
ISSN 02-1226, CN 11-1706

Chinese Science Bulletin
Volume 56, Number 12, December 2014
ISSN 02-1226, CN 11-1706

Chinese Science Bulletin
Volume 56, Number 1, January 2015
ISSN 02-1226, CN 11-1706



Chinese Science Bulletin

A multidisciplinary scientific journal
Published three times every month

Print ISSN: 1001-6538
Online ISSN: 1861-9541

- Peer-reviewed
- Online submission
- Indexed by SCI, CA, etc.
- Professional and quick publication
- Pub ASAP

Editorial Office

Managing Editors

AN Rui (Director) ZHANG Li (Vice Director)

Editorial Staff

- LIN Lin (linlin@scichina.org)
- SUN HongMei (shm@scichina.org)
- WANG Jing (wangj@scichina.org)
- WANG YuanHuo (wyh@scichina.org)
- ZHAO FengChao (fengchao@scichina.org)
- ZHI Xin (zhixin@scichina.org)
- ZOU WenJuan (zouwenjuan@scichina.org)

● Cover designed by HU Yu.

Address:

16 Donghuangchenggen North Street, Beijing 100717, China

Tel: +86-10-64036120 Fax: +86-10-64016350

Email: csb@scichina.org

Sponsored by
Chinese Academy of Sciences (CAS)
National Natural Science Foundation of China (NSFC)

Published by
Science China Press & Springer

ISSN 1001-6538

